Supporting Information

Fully Transparent, Flexible and Waterproof Synapses with Pattern Recognition in Organic Environment

Tian-Yu Wang[1], Jia-Lin Meng[1], Zhen-Yu He[1], Lin Chen[1]*, Hao Zhu[1], Qing-Qing Sun[1]*, Shi-Jin Ding[1], Peng Zhou[1], and David Wei Zhang[1]

[1]State Key Laboratory of ASIC and System, School of Microelectronics, Fudan University, Shanghai 200433, China

*Correspondence and requests for materials should be addressed to L.C. and Q.Q.S. (E-mail : linchen@fudan.edu.cn; qqsun@fudan.edu.cn;)

S1. Current response with time according to the applied pulses.

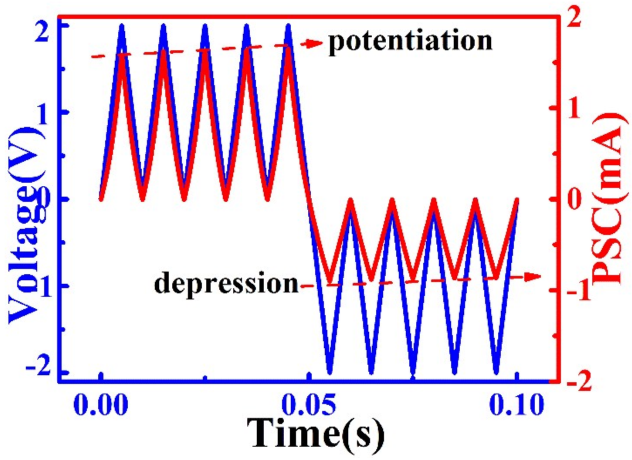

Figure S1. Potentiation and depression of e-synapse under consecutive pulses. The PSC response with the consecutive pre-synaptic spikes, including 5 positive spikes of 2V and 5 negative spikes of -2V. The spikes width are all 10ms. The blue curves are the voltage used in the operation process and the red curves are the current response with applied voltage. The instant current of post synapse increased monotonically with the increase of applied positive spikes number while decreased with the increase of negative spikes number, indicating the potentiation and depression potential for modulated conductance of e-synapse. The characteristics are similar to the nonlinear transmission behaviors in bio-synapses.

S2. EPSC and IPSC of artificial synaptic devices.

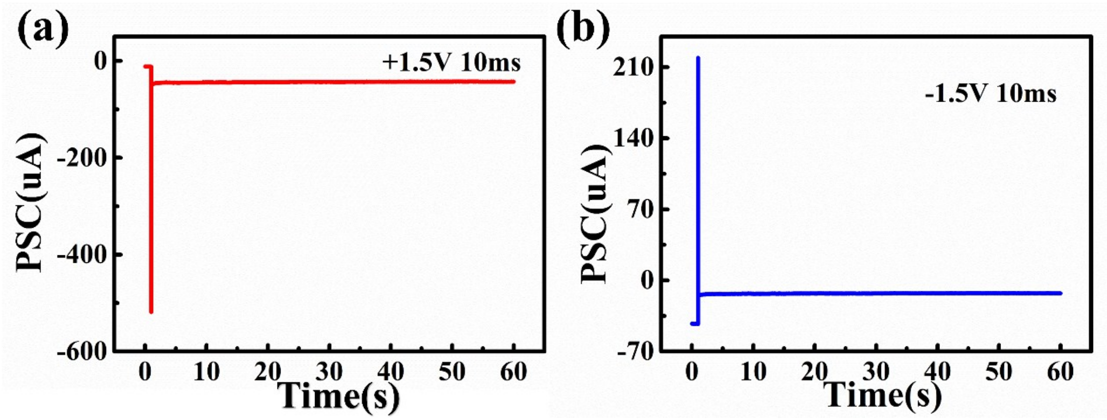

Figure S2. EPSC and IPSC behaviors in e-synapses. (a) Excitatory postsynaptic current (EPSC) induced by a single bias pulse of 1.5V with the duration of 10ms, which is the basis of LTP with consecutive pulses.[1,2] The PSC after pulse was larger than initial state in excitatory behavior, corresponding to the excitatory signal transmission in bio-synapse. (b) Inhibitory postsynaptic current (IPSC) with voltage pulse stimulation (-1.5V, 10ms). The process simulating the inhibitory signal transmission between two connected neurons.

S3. Potentiation and depression pulse operation for LTP and LTD.

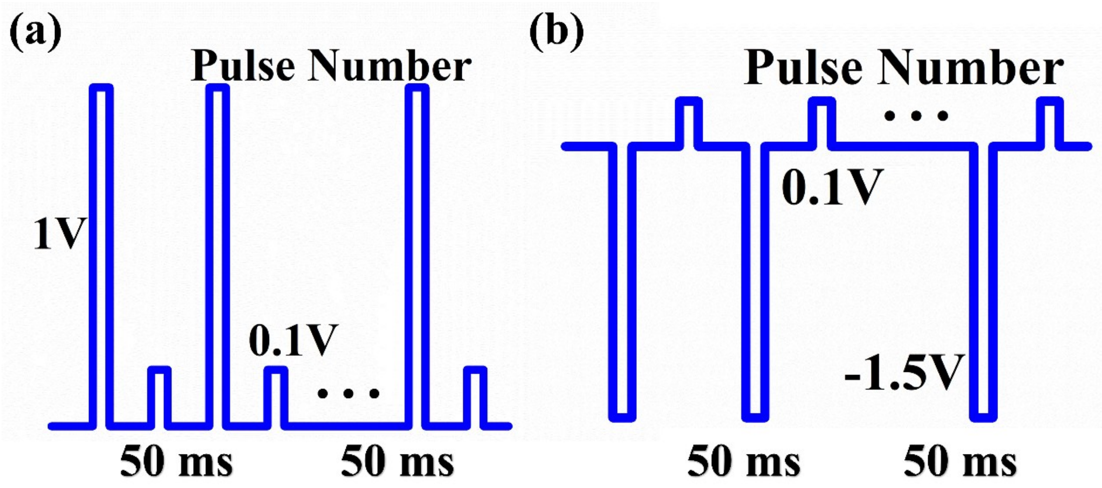

Figure S3. Schematic diagram of the operation pulses. (a) The positive pulses sequence, including operated spikes followed by read spikes. During the process of simulating LTP, consecutive positive spikes (pulse width of 50ms, pulse amplitude of 1V) were applied to the artificial synapse. The read voltage is 100mV after operating pulses without influencing the conductance states. (b) Negative spikes used for the emulation of LTD behavior in e-synapse. The consecutive pulses an operation spike and a small read spike, which are -1.5V/50ms and 0.1V/50ms in one cycle, respectively. There were 600 cycles in the process of LTP and LTD totally for electrical long-term plasticity.

S4. The fitting result of normalized conductance and normalized number of pulses.

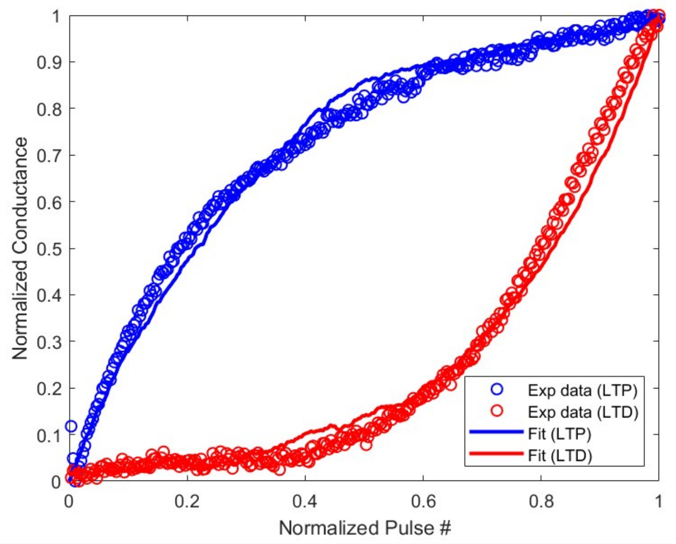

Figure S4. The fitting of nonlinearity coefficient alpha of long-term potentiation (α_p) and depression (α_d) in our device. The results where α_p=3.5 and α_d=-4.1 were fitted using a device behavioral mode with the following equations.

$$G_p = B\left(1 - e^{-\frac{P}{A_p}}\right) \tag{1}$$

$$G_d = -B(1 - e^{-\frac{P - P_{max}}{A_d}}) \tag{2}$$

$$B = (G_{max} - G_{min})/(1 - e^{-\frac{-P_{max}}{A_{d,p}}}) \tag{3}$$

where G_p and G_d are the conductance of device during potentiation and depression, respectively. G_{max} and G_{min} represent the maximum and minimum conductance during weights update, respectively. P is the pulse number and A is the parameter that controls the nonlinear behavior in LTP/LTD.

S5. Mechanism of our artificial synaptic device.

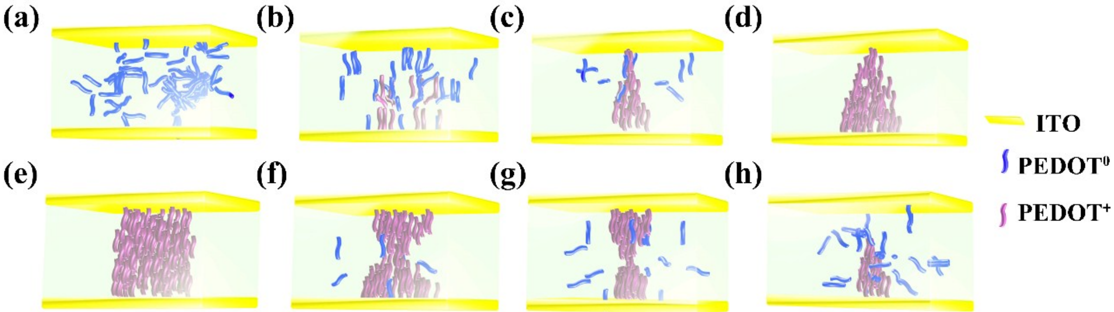

Figure S5. The hole injection ($PEDOT^0 + h^+ \rightarrow PEDOT^+$) occurred when the positive voltage was applied to the top electrode. In LTP process, the conductive trap of $PEDOT^+$ accumulated to form conductive filaments, which caused an increase of conductance. In LTD process, the conductance of the device gradually decreased under negative pulses due to the shift of $PEDOT^+$ to $PEDOT^0$, which destroyed the conductive filaments.

S6. The relearning behaviors for 10 times in e-synapses.

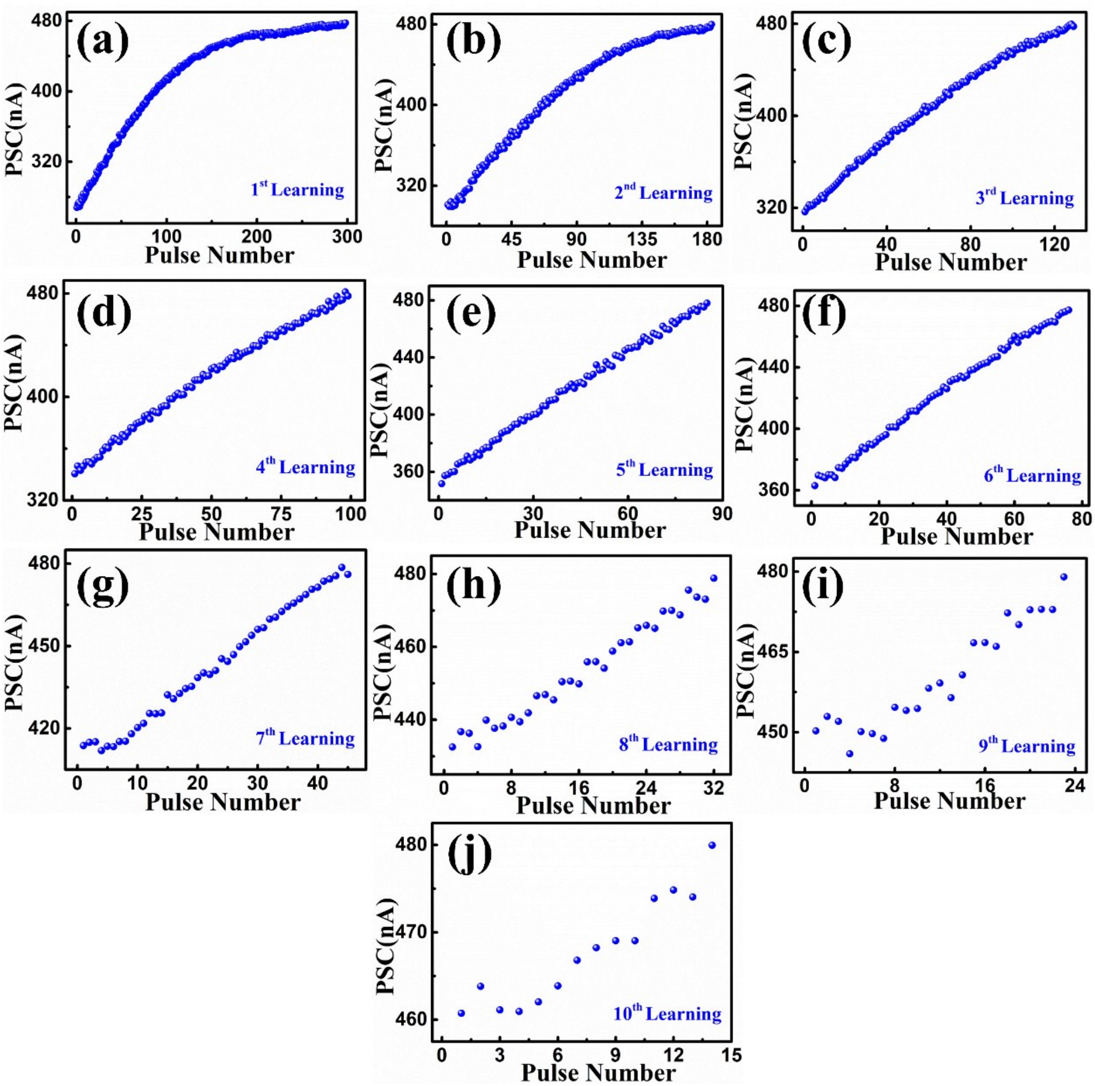

Figure S6. The learning processes with different times. (a) The first learning process of a fresh device. It takes 300 pulses to realize the memory function. (b) The 2th learning process after decayed spontaneously of first learning, which needs 183 pulses. (c) The 3rd learning process takes 129 pulses to recover to the end level of last learning process. (d)- (j) The 4th, 5th, 6th, 7th, 8th, 9th and 10th learning process with 85 pulses, 76 pulses, 45 pulses, 32 pulses, 23 pulses and 14 pulses, respectively. All the pulses under different times could take the device to initial learning level. With the increase of learning times, the spikes need for recovery decreased. The phenomenon is close similarly to the relearning behaviors in brain, which relearns forgotten information more quickly than the former learning process.[3-5]

S7. The 10th forgetting state of device.

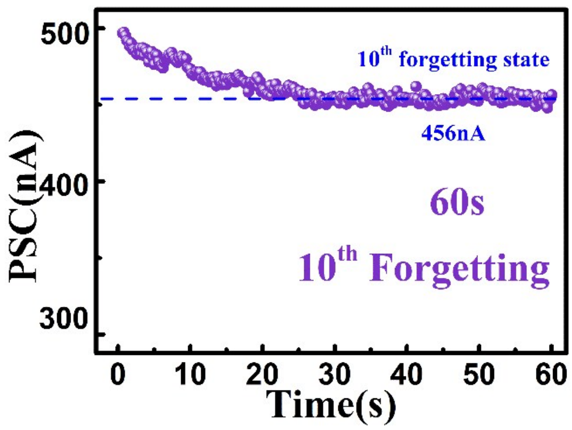

Figure S7. The post-synaptic current was monitored for 60s after 10th learning process. The stable current increased from 309nA of first forgetting behavior to 456nA of 10th forgetting behavior, indicating the learning–experience behavior in our artificial synaptic device.

S8. Flowchart of the training process for pattern recognition.

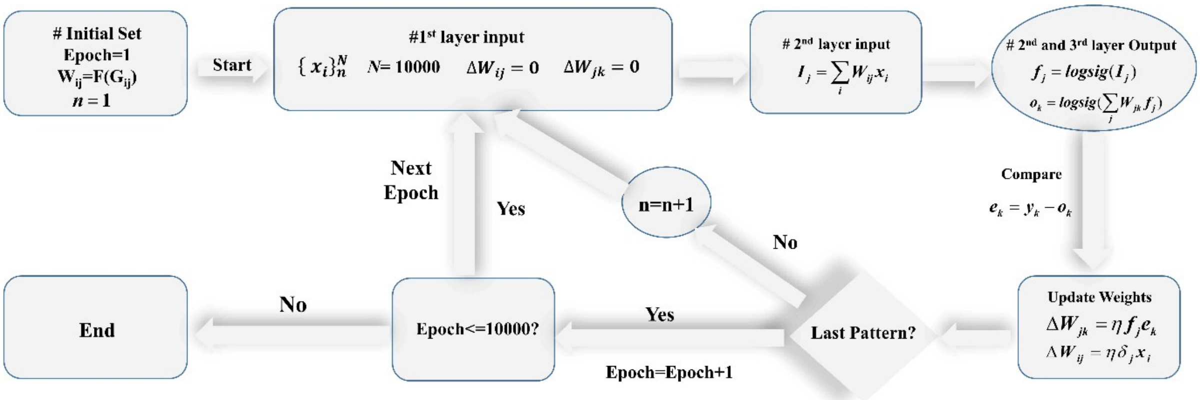

Figure S8. Flowchart of training algorithm, where W_{ij} is the synaptic weights, G_{ij} is the conductance of synaptic device, N is the sample number of training patterns and ΔW_{jk} represents the altering value for weights update. The input signal of hidden layer is $I_j(n) = \sum_{i=1}^{256} W_{ij} x_i(n)$, which could be activated by log-sigmoid (logsig) function. The output signal of hidden layer and 3rd layer is $f_j(n) = logsig(I_j)$ and $O_k = logsig(\sum_j W_{jk} f_j)$, respectively. By comparing the real and target output value, the altering value of ΔW_{ij} and ΔW_{jk} were determined and transferred to the 1st layer for weights update. After all images were input for training, one epoch for pattern recognition was finished.

S9. The output signals of training and testing images.

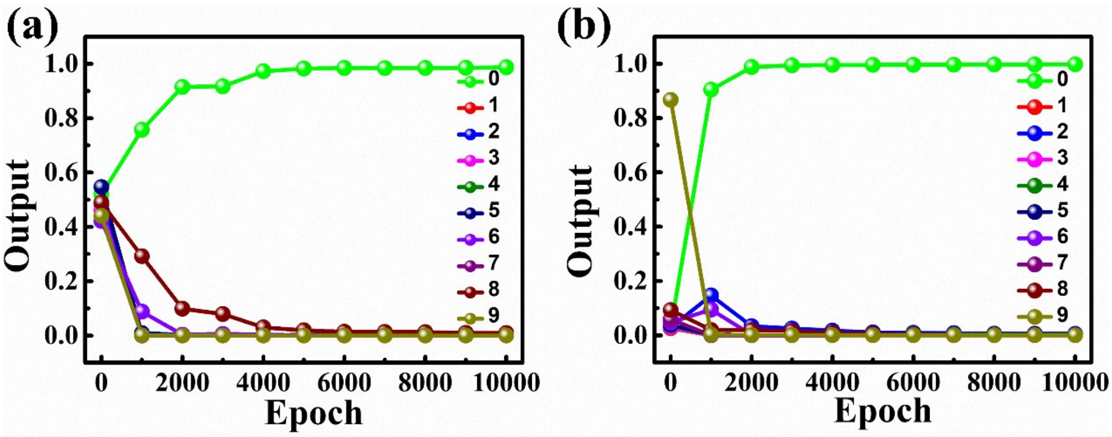

Figure S9. The output signals in the 10000 epoch for training and testing images. (a) The output signals of 10000 training images from “0” to “9”. The results show that the neuron network could recognize the digit of “0” from the other digits easily and remain stable recognition after 2000 epoch. (b) The output signals of 500 testing images from “0” to “9”. The neuron network based on our synaptic device took “9” as “0” before training and could select the digit of “0” successfully after 1500 epoch. To ensure the reliability of recognition rate, the neuron network needs at least 2000 epoch for training.

S10. The recognition rate with different hidden layers.

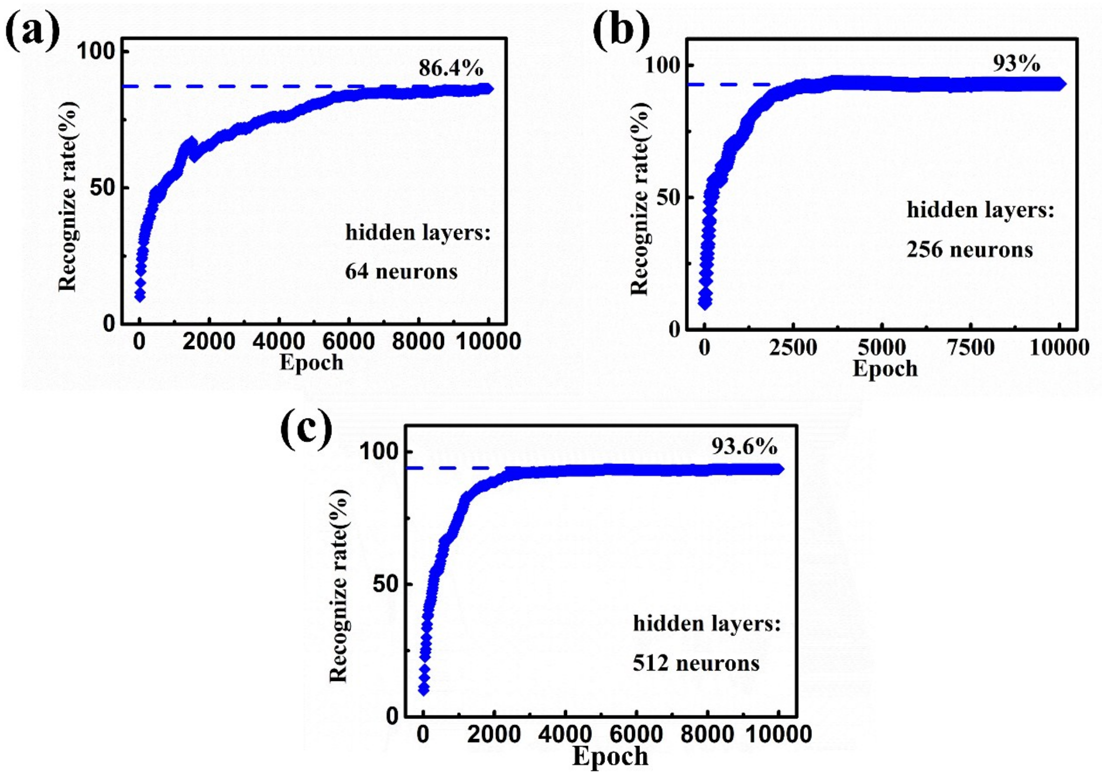

Figure S10. The recognition rate of different neuron network. (a) The recognition rate of hidden layer with (a) 64 neurons, (b) 256 neurons and (c) 512 neurons could achieve 86.4%, 93% and 93.6% after 10000 training epoch, respectively. The different neurons in hidden layer could affect the final recognition accuracy. In this work, 128 neurons were simulated for pattern recognition with the accuracy of 92.4%, which is enough for recognition applications and could simplify simulation in artificial neuromorphic computing system.

S11. The photograph of synaptic device in different organic solvents.

Figure S11. Images of e-synapses being immersed in different solutions. The artificial synaptic device was treatment in (a) ethanol, (b) acetone, (c) DMF, (d) methanol and (e) toluene. It was immersed in every sort of organic solvents for 12 hours. After immersing, there was no obvious change of the device with electrodes of different diameters and the e-synapse could stable work with 6000 spikes after removing from these solutions. Our device showed reliable characteristics and paved the way for short-term applications in organic environment.

References

1. Z. Q. Wang, H. Y. Xu, X. H. Li, H. Yu, Y. C. Liu and X. J. Zhu, *Adv. Funct. Mater.*, 2012, **22**, 2759-2765.
2. Q. Lai, L. Zhang, Z. Li, W. F. Stickle, R. S. Williams and Y. Chen, *Adv. Mater.*, 2010, **22**, 2448-2453.
3. J. Choi, J. S. Han, K. Hong, S. Y. Kim and H. W. Jang, *Adv. Mater.*, 2018, **30**, 1704002.

4. M. Yang, X. Zhao, Q. Tang, N. Cui, Z. Wang, Y. Tong and Y. Liu, *Nanoscale*, 2018, **10**, 18135-18144.
5. Y. Park and J. Lee, *ACS Nano*, 2017, **11**, 8962-8969.